Contents lists available at ScienceDirect

Computational Biology and Chemistry

journal homepage: www.elsevier.com/locate/compbiolchem

In silico analysis of EST and genomic sequences allowed the prediction of *cis*-regulatory elements for *Entamoeba histolytica* mRNA polyadenylation

Absalom Zamorano[a], César López-Camarillo[b], Esther Orozco[c], Christian Weber[d,e], Nancy Guillen[d,e], Laurence A. Marchat[a,*]

[a] *ENMH-IPN, Programa Institucional de Biomedicina Molecular, Guillermo Massieu Heguera #239, Ticoman, CP 07320, México, D.F., Mexico*
[b] *Universidad Autónoma de la Ciudad de México, Posgrado en Ciencias Genómicas, Av. San Lorenzo #290, Col. del Valle, CP 03100, México, D.F., Mexico*
[c] *CINVESTAV-IPN, Departamento de Patología Experimental, Av. IPN # 2508, Col. San Pedro Zacatenco, CP 07360, México, D.F., Mexico*
[d] *Institut Pasteur, Unité Biologie Cellulaire du Parasitisme, 28 rue du Dr. Roux, Paris F-75015, France*
[e] *INSERM U786, Paris F-75015, France*

ARTICLE INFO

Article history:
Received 12 September 2007
Received in revised form 24 March 2008
Accepted 24 March 2008

Keywords:
Bioinformatics analysis
Pre-mRNA 3′-end processing
Cis-regulatory elements
Protozoan parasite

ABSTRACT

In most eukaryotic cells, the poly(A) tail at the 3′-end of messenger RNA (mRNA) is essential for nuclear export, translatability, stability and transcription termination. Poly(A) tail formation involves multiprotein complexes that interact with specific sequences in 3′-untranslated region (3′-UTR) of precursor mRNA (pre-mRNA). Here we have performed a computational analysis of a large EST and genomic sequences collection from *Entamoeba histolytica*, the protozoan parasite responsible for human amoebiasis, to identify conserved elements that could be involved in pre-mRNA polyadenylation. Results evidenced the presence of an AU-rich domain corresponding to the consensus UA(A/U)UU polyadenylation signal or variants, the cleavage and polyadenylation site that is generally denoted by U residue and flanked by two U-rich tracts, and a novel A-rich element. This predicted array was validated through the analysis of genomic sequences and predicted mRNA folding of genes with known polyadenylation site. The molecular organization of pre-mRNA 3′-UTR *cis*-regulatory elements appears to be roughly conserved through evolutionary scale, whereas the polyadenylation signal seems to be species-specific in protozoan parasites and the novel A-rich element is unique for the primitive eukaryote *E. histolytica*. To our knowledge, this paper is the first work about the identification of potential pre-mRNA 3′-UTR *cis*-regulatory sequences through in silico analysis of large sets of cDNA and genomic sequences in a protozoan parasite.

1. Introduction

The knowledge of parasite genome sequences is an extraordinary tool to identify and functionally characterize new genes that are important for pathogen survival and host infection. It also makes possible the determination of genes organization and the detection of conserved *cis*-regulatory elements for gene expression. Experimental characterization of 5′- and 3′-untranslated regions (5′-UTR and 3′-UTR, respectively) successfully allows the identification of control sequences, but they are usually limited to a small number of genes and specific contextual scopes. Moreover, they often consider individual interactions without taking surrounding sequences or factors into account. Computational analysis of genomic, full-length cDNA and expressed sequence tag (EST) databases represents an attractive alternative to detect conserved signals that can be important for the expression of numerous genes.

Bioinformatics approach has been largely used to predict regulatory elements for precursor messenger RNA (pre-mRNA) 3′-end polyadenylation (Beaudoing et al., 2000; Hajarnavis et al., 2004; Loke et al., 2005) that is a crucial maturation step for most eukaryotic mRNA, affecting stability, translatability, and nuclear-to-cytoplasmic export (Zhao et al., 1999), representing therefore an integral part of gene expression regulation. The polyadenylation reactions involves about 25 nuclear proteins that recognize poly(A) sequences in pre-mRNAs 3′-UTR and act in a coordinated way to perform polyadenylation reaction (Proudfoot, 2004). In human cells and yeast, the polyadenylation site (poly(A) site) is generally flanked by the upstream polyadenylation signal (A(A/U)UAAA) and the downstream U/GU-rich element. Additional U-rich and G/C-rich elements are also associated with poly(A) site (Zhao et al., 1999; Graber et al., 2002; Hu et al., 2005).

Entamoeba histolytica is the intestinal protozoan parasite responsible for amebic colitis and liver abscess, which cause

* Corresponding author. Tel.: +52 55 5729 6300x55543.
E-mail address: l_marchat@yahoo.com.mx (L.A. Marchat).

1476-9271/$ – see front matter © 2008 Elsevier Ltd. All rights reserved.
doi:10.1016/j.compbiolchem.2008.03.019

mortality in many developing countries (Jackson, 2000). The sequencing of the parasite genome provides new insights into the cellular workings and genome evolution of this major human pathogen (Loftus et al., 2005). As a first step towards characterizing 3′-UTR *cis*-regulatory sequences that could be important for pre-mRNA 3′-end processing in *E. histolytica*, we performed a small-scale in silico analysis of genomic regions and identified four conserved motifs (López-Camarillo et al., 2005). Here, we extended the computational analysis to a larger *E. histolytica* EST collection and genomic sequences dataset and proposed a hypothetical array of UA(U/A)UU, U-rich and A-rich elements in pre-mRNA 3′-UTR. Finally, our model was validated by studying genomic sequences and secondary RNA structures of *E. histolytica* genes with known poly(A) site.

2. Materials and methods

2.1. Sequences selection

E. histolytica EST were selected from a set of 2348 raw cDNA sequences obtained by retrotranscription of mRNA isolated from the virulent HM1:IMSS strain. Briefly, cDNA sequences were generated by reverse transcription initiated by an oligodeoxythymidylate primer, cloned into the TriplRx2M plasmid (Clontech) and automatically sequenced (Weber et al., 2006). As the cloning strategy was not oriented, sequences were searched for the presence of at least ten A or T residues tracts that were assumed to correspond to EST 3′-ends. For sequences with poly(T) tract, we obtained complementary strands and inverted them, so that they were in sense orientation. To eliminate sequences with internal poly(A) tracts and make certain of working with 3′-ends, we selected sequences having at least 400 nucleotides (nt) upstream the 10-A tract and cut them to conserve the last 100 bases at the 3′-end. Finally, sequences were checked for redundancy by intersequence comparisons. Any pair of sequences with identity greater than 90% was considered as the same transcript and one was eliminated from the data set. Therefore, assuming no errors, the 3′-end of the selected EST sequences were considered as the poly(A) site.

Genomic sequences were obtained from *E. histolytica* genome databases (http://www.tigr.org/tdb/e2k1/eha1/ and http://www.sanger.ac.uk/Projects/E_histolytica/). Loci were randomly chosen throughout the parasite genome to retrieve nt sequence of selected open reading frames (ORFs) including 3′-UTR. This information was used to select DNA sequences corresponding to 180 nt around the predicted stop codon in order to conserve 60 bases of ORF and 120 nt of 3′-UTR for each locus. Finally, sequences were checked for redundancy as described above.

2.2. Sequences analysis of EST and genomic sequences

As we were looking for elements involved in pre-mRNA 3′-end formation, T residues were substituted by U residues in both EST and genomic sequences. Entropy and single nt frequencies were determined using the bioinformatics tools of the BioEdit biological sequences alignment editor (version 7.0.5.3) (http://www.mbio.ncsu.edu/BioEdit/bioedit.html). To identify potential *cis*-regulatory elements, we obtained all the strings of size four, five and six, formed by A, C, U, G and N (where N is any nt) and sequences were screened for all 4-nt, 5-nt and 6-nt words by brute force string search to find those with the largest frequency. In EST and genomic sequences, motifs position was expressed in relation to the poly(A) site and the stop codon, respectively, which were arbitrarily fixed at position 0. Finally, we used the Quikfold program at http://www.bioinfo.rpi.edu/applications/hybrid/quikfold.php (Zuker, 2003; Markham and Zuker, 2005) to predict transcripts folding for genes with known poly(A) site using defaults parameters

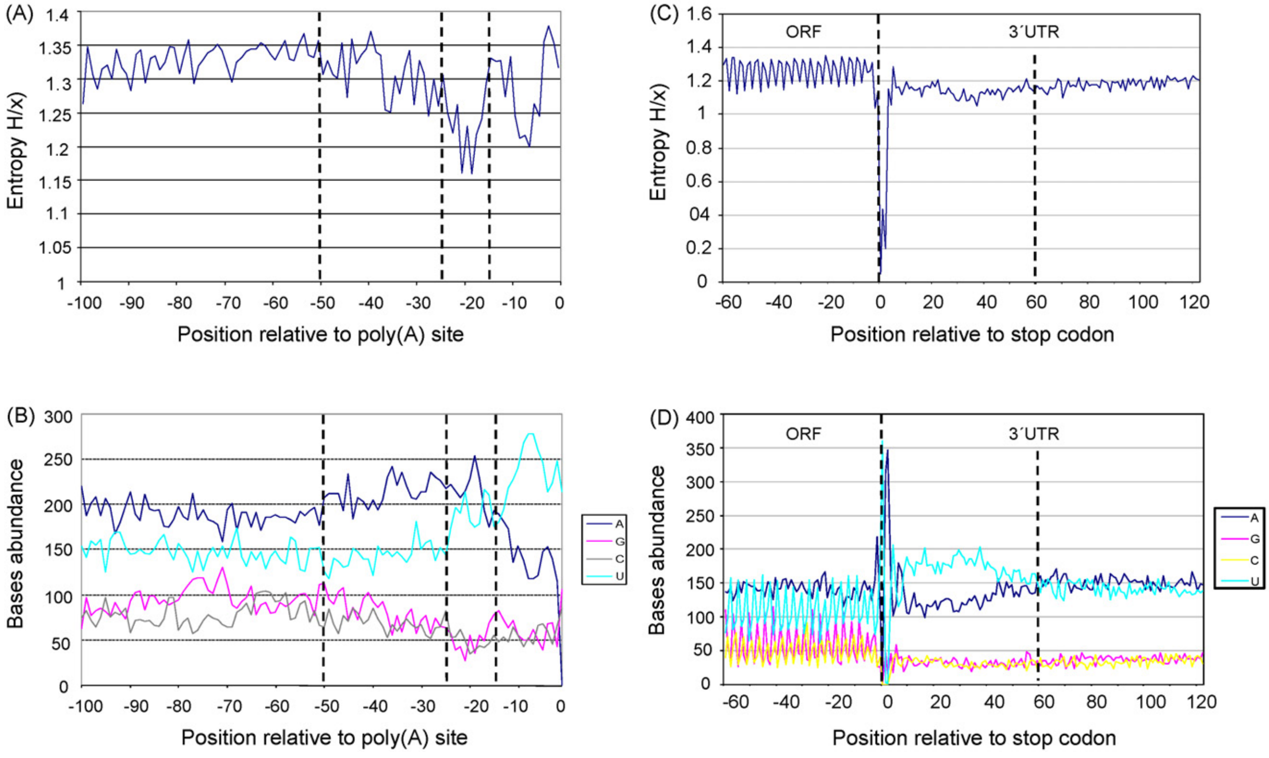

Fig. 1. Nucleotide analysis of *E. histolytica* EST (A and B) and genomic (C and D) sequences. (A and C) Entropy determination. (B and D) Single-nucleotide frequencies. Positions are relative to potential poly(A) site and stop codon (position 0) in EST and genomic sequences, respectively. Discontinuous lines delimit domains characterized by similar enthropy value and nucleotide content.

(37 °C, 1 M [Na^{2+}] and 0 M [Mg^{2+}]); top free energy value was considered to select the most probable structures.

3. Results

3.1. Identification of conserved regions in 3′-end of E. histolytica cDNA sequences

The initial set of 2348 raw cDNA sequences was submitted to successive filtering processes to select EST sequences whose 3′-end was considered as the poly(A) site (position 0). The last 100 nt of the resulting 512 cDNA sequences were then examined for information content through the determination of entropy that is a measure of the uncertainty associated with a random variable. In this approach, information entropy is thought to provide data about the amount of nt variability at each position relative to the poly(A) site in the set of aligned sequences, allowing the measure of the information content at each nt position in the alignment. As shown in Fig. 1A, cDNA sequences could be roughly divided in two distinct regions. From −100 to −50 nt, entropy values were high (mean value: 1.3286), indicating a lack of predictability at an aligned position that is probably due to the fact that this region corresponds to distinct ORF without any conserved motifs. In contrast, entropy values decreased in the last 50 nt towards the poly(A) site (mean value: 1.2887), indicating a higher information content. Remarkably, the entropy plot evidenced three windows spanning from −50 to −25 nt (minimum value: 1.2449), −25 to −15 nt (minimum value: 1.1592) and −15 nt to poly(A) site (minimum value: 1.1991), respectively (Fig. 1A), that could correspond to three conserved domains.

The 512 ESTs were then examined for single nt frequencies at each position relative to the poly(A) site (Fig. 1B). Sequences upstream the poly(A) site generally presented an AU-rich content, with an average A and U residues frequency around 37% and 32%, respectively. A detailed examination of curves revealed four distinct regions: from −100 to −50 nt, nt content was almost constant; from −50 to −25 nt, the abundance of A increased, whereas the U content was kept almost unchanged and GC content decreased; from −25 to −15 nt, sequences displayed a combination of A and U residues that could correspond to the UA(A/U)UU polyadenylation signal; and the last 15 nt-region preceding the poly(A) site exhibited a clear peak of U residues. Finally, the last nt at 3′-end was a U residue in more than 40% of EST sequences, suggesting that it is the preferred poly(A) site (Fig. 1B). Interestingly, these four regions were in agreement with those previously determined from the information content analysis (Fig. 1A), confirming their significance.

3.2. Identification of conserved regions in 3′-end of E. histolytica genomic sequences

363 distinct loci were obtained from the parasite genome databases and filtered before evaluating information content and single nt frequencies throughout a180 nt-region around the predicted stop codon (position 0) (Fig. 1C). Entropy profile confirmed the existence of differences between codifying and not codifying regions, the mean entropy value being higher (1.2609) in the 60 nt region upstream the stop codon than in the last 120 nt (1.1549). This confirmed the lack of predictability at an aligned position in distinct ORF and indicated an higher information content in 3′-UTR. Interestingly, entropy values dramatically decreased down to 0.04786 at position 0, in agreement with the relevance of the stop codon. Although the entropy plot did not evidence any specific regions with high information content in 3′-UTR, values were lower throughout the first 60 nt, suggesting the presence of informative elements near the stop codon (Fig. 1C).

Table 1
Classification of EST sequences according to the number of consensus UAAUU and UAUUU polyadenylation signals

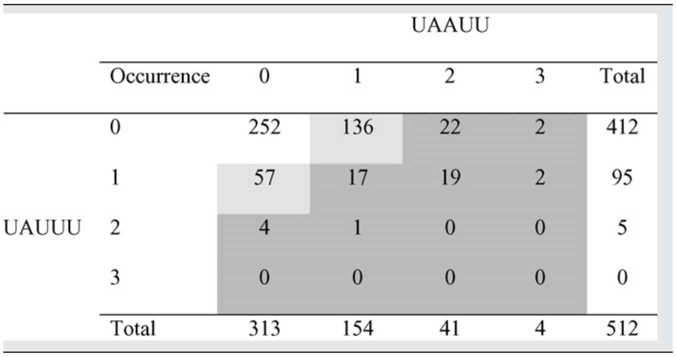

		UAAUU				
	Occurrence	0	1	2	3	Total
UAUUU	0	252	136	22	2	412
	1	57	17	19	2	95
	2	4	1	0	0	5
	3	0	0	0	0	0
	Total	313	154	41	4	512

White cell, sequences without any consensus polyadenylation signal; light grey cell, sequences with a single consensus polyadenylation signal; dark grey cell, sequences with multiple consensus polyadenylation signals.

Next, we examined the same genomic sequences for single nt frequencies at each position relative to the stop codon (Fig. 1D). The AU content was higher in 3′-UTR (81%) that in coding regions (70%) as previously reported (López-Camarillo et al., 2005). After the stop codon, we observed a short strength of AU residues (4–10 nt) followed by a 50-nt region with a disproportionate frequency of U residues, whereas there was a combination of AU residues and a low GC content throughout the last 60 nt. Remarkably, the A-rich region previously identified from EST analysis was detected upstream the stop codon showing that it did not correspond to a 3′-UTR conserved motif but was located inside codifying sequences (Fig. 1D). Based on results obtained from EST and genomic DNA sequences analysis, we proposed that potential regulatory elements could be located in the 25 nt-region upstream the poly(A) site and in the 60 nt-region downstream the stop codon.

3.3. Identification of conserved elements in 3′-end of E. histolytica cDNA sequences

In order to identify the conserved motifs located before the poly(A) site, we searched for the most representative words located in the last 25 nt of the EST collection. We initially focused on 5-nt motifs because the only reported 3′-end processing element in *E. histolytica* is the consensus UA(U/A)UU polyadenylation signal (Bruchhaus et al., 1993) (Table 1). A single UAAUU or UAUUU motif was present in 136 (27%) and 57 (11%) sequences, respectively. 68 (13%) sequences presented various UA(U/A)UU motifs, while 252 (49%) sequences did not present UAAUU nor UAUUU motifs.

When we analyzed the global frequency score of the top-10 motifs present at least once in the EST set (Fig. 2A), the UAAUU signal appeared at the 2nd place, whereas the UAUUU motif was at the 13th place (Supplementary Fig. 1). Other recurrent pentamers, such as UUAUU (7th) and AAUUU (9th), could be variants of the reported polyadenylation signals with a single nt changed. The other AU-rich motifs (UUAAU, AUUAA and AAUUA), have more than one substitution. The UUUUU word appeared as the most global common motif, in agreement with the high U content in EST sequences. Considering that words with 4 o 5 U residues are U-rich motifs, we proposed that UUAUU (7th), AUUUU (8th) and UUUUA (10th), together with the UUUUU pentamer, could contribute to the formation of the U-rich region identified in Fig. 1B. Although its high abundance, the AAAA motif (4th) was not considered as relevant since it is the only A-rich word detected (Fig. 2A and Supplementary Fig. 1). Analysis of

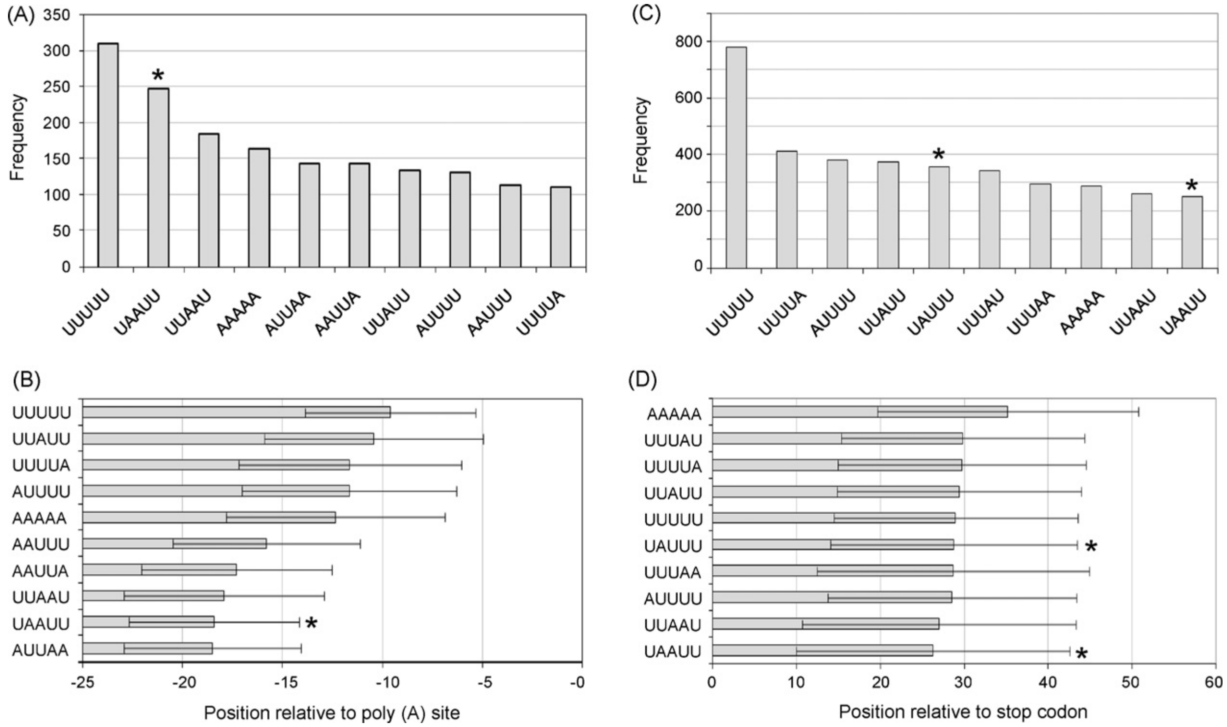

Fig. 2. Identification of the ten most abundant pentamers in *E. histolytica* EST (A and B) and genomic (C and D) sequences. (A and C) Global occurrence frequency. (B and D) Position. Star, conserved UA(U/A)UU polyadenylation signal. Positions are relative to potential poly(A) site and stop codon (position 0) in EST and genomic sequences, respectively.

4-nt and 6-nt words occurrence frequencies did not identify other relevant motifs (data not shown).

We next analyzed the relative position of the most representative 5-nt words identified above (Fig. 2B). Interestingly, AU-rich motifs were centered on −18 to −16 nt positions, excepted the UUAAU motif that clustered with U-rich motifs around −13 to −9 nt positions. Both regions matched with those previously identified (Fig. 1A and B).

3.4. *Identification of conserved elements in 3′-end of E. histolytica genomic sequences*

To characterize 3′-UTR after the poly(A) site, we searched for the most representative 5-nt words in the 60 nt region downstream the stop codon in genomic sequences (Table 2). A single consensus polyadenylation signal, UAAUU or UAUUU, was detected in 46 (13%) and 69 (19%) sequences, respectively. Multiple consensus polyadenylation signal were detected in 188 (52%) genomic sequences, whereas 61 (17%) genes did not have UAAUU nor UAUUU motifs.

Analysis of the global frequency score of the top-10 motifs present at least once in genomic sequences (Fig. 2C), showed that the consensus UAUUU and UAAUU motifs appeared at the 5th and 10th place, respectively. The UUAUU motif that was proposed above to be a variant of the consensus polyadenylation signals with a single nt changed, was at the 4th place, whereas the other recurrent AU-rich motifs with various substitutions, UUUAA and UUAAU, were at the 7th and 9th position, respectively. The UUUUU word (1st) together with other U-rich words, UUUUA, AUUUU, UUAUU, UAUUU and UUUAU (2nd–6th place), contributed to the high U

Table 2
Classification of genomic sequences according to the number of consensus UAAUU and UAUUU polyadenylation signals

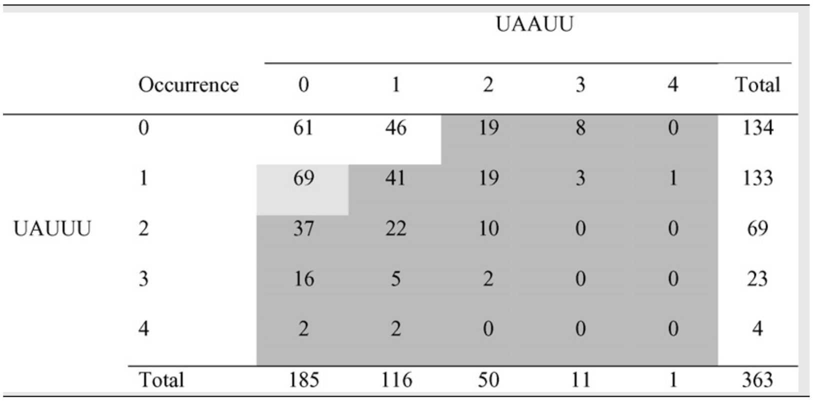

		UAAUU					
	Occurrence	0	1	2	3	4	Total
UAUUU	0	61	46	19	8	0	134
	1	69	41	19	3	1	133
	2	37	22	10	0	0	69
	3	16	5	2	0	0	23
	4	2	2	0	0	0	4
	Total	185	116	50	11	1	363

White cell, sequences without any consensus polyadenylation signal; light grey cell, sequences with a single consensus polyadenylation signal; dark grey cell, sequences with multiple consensus polyadenylation signals.

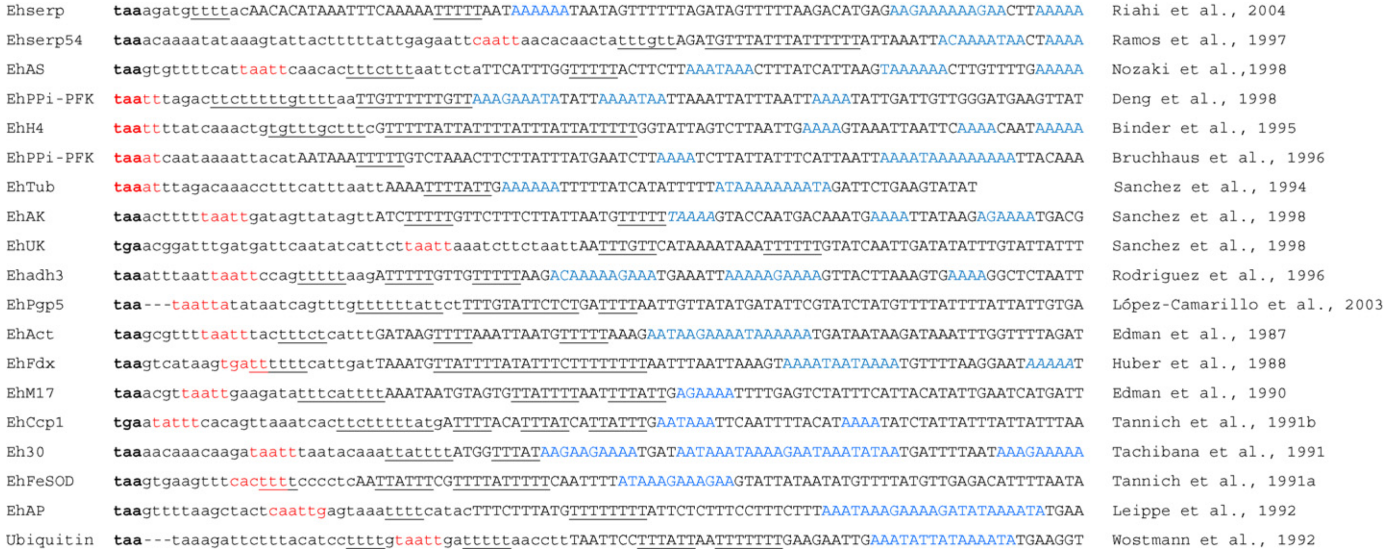

```
Ehserp      taaagatgttttacAACACATAAATTTCAAAAATTTTTAATAAAAAATAATAGTTTTTAGATAGTTTTTAAGACATGAGAAGAAAAAAGAACTTAAAAA   Riahi et al., 2004
Ehserp54    taaacaaaatataaagtattactttttattgagaattcaattaacacaactatttgttAGATGTTTATTTATTTTTTATTAAATTACAAAATAACTAAAA   Ramos et al., 1997
EhAS        taagtgttttcattaattcaacacttctttaattctaTTCATTTGGTTTTTACTTCTTAAATAAACTTTATCATTAAGTAAAAAACTTGTTTTGAAAAA   Nozaki et al.,1998
EhPPi-PFK   taatttagacttcttttgttttaaTTGTTTTTTGTTAAAGAAATATATTAAAATAATTAAATTATTTAATTAAAATATTGATTGTTGGGATGAAGTTAT   Deng et al., 1998
EhH4        taatttatcaaactgtgtttgctttcGTTTTATTATTTTATTTATTATTTTTGGTATTAGTCTTAATTGAAAAGTAAATTAATTCAAAACAATAAAAA   Binder et al., 1995
EhPPi-PFK   taaatcaataaaattacatAATAAATTTTTGTCTAAACTTCTTATTTATGAATCTTAAAATCTTATTATTTCATTAATTAAAATAAAAAAAAATTACAAA   Bruchhaus et al., 1996
EhTub       taaatttagacaaacctttcatttaattAAAATTTTATTGAAAAAATTTTTATCATATTTTTATAAAAAAAAATAGATTCTGAAGTATAT              Sanchez et al., 1994
EhAK        taaacttttaattgatagttatagttATCTTTTTGTTCTTTCTTATTAATGTTTTTTAAAAGTACCAATGACAAATGAAAATTATAAGAGAAAATGACG   Sanchez et al., 1998
EhUK        tgaacggatttgatgattcaatatcattcttaattaaatcttctaattAATTTGTTCATAAAATAAATTTTTTGTATCAATTGATATATTTGTATTATTT   Sanchez et al., 1998
Ehadh3      taaatttaattaattccagttttaagATTTTTGTTGTTTTTAAGACAAAAAGAAATGAAATTAAAAAGAAAAGTTACTTAAAGTGAAAAGGCTCTAATT   Rodriguez et al., 1996
EhPgp5      taa---taattatataatcagtttgtttttattctTTTGTATTCTCTGATTTTAATTGTTATATGATATTCGTATCTATGTTTTATTTTATTATTGTGA   López-Camarillo et al., 2003
EhAct       taagcgttttaatttactttctcatttGATAAGTTTTAAATTAATGTTTTTAAAGAATAAGAAAATAAAAAATGATAATAAGATAAATTTGGTTTTAGAT   Edman et al., 1987
EhFdx       taagtcataagtgattttttcattgatTAAATGTTATTTTATATTTCTTTTTTTTAATTTAATTAAAGTAAAATAATAAAATGTTTTAAGGAATAAAAAT   Huber et al., 1988
EhM17       taaacgttaattgaagatatttcatttAAATAATGTAGTGTTATTTTAATTTTATTGAGAAAATTTTGAGTCTATTTCATTACATATTGAATCATGATT   Edman et al., 1990
EhCcp1      tgaatatttcacagttaaatcacttcttttatgATTTTACATTTATCATTATTTGAATAAATTCAATTTTACATAAAATATCTATTATTTATTATTTAA   Tannich et al., 1991b
Eh30        taaaacaaacaagataatttaatacaaattatttATGGTTTATAAGAAGAAAATGATAATAAATAAAAGAATAAATATAATGATTTTAATAAAGAAAAA   Tachibana et al., 1991
EhFeSOD     taagtgaagtttcacttttcccctcAATTATTTCGTTTTATTTTTCAATTTTATAAAGAAAGAAGTATTATAATATGTTTTATGTTGAGACATTTTAATA   Tannich et al., 1991a
EhAP        taagttttaagctactcaattgagtaaatttcatacTTTCTTTATGTTTTTTTTATTCTCTTTCCTTTCTTTAAATAAAGAAAAGATATAAAATATGAA   Leippe et al., 1992
Ubiquitin   taa---taaagattctttacatcctttgtaattgattttaaccttTAATTCCTTTATTAATTTTTTTGAAGAATTGAAATATTATAAAATATGAAGGT   Wostmann et al., 1992
```

Fig. 3. Analysis of DNA sequences downstream the stop codon of genes with experimentally determined poly(A) site. The conserved motifs predicted by our in silico analysis are indicated as follow: bold, stop codon; red, polyadenylation signal; underlined, U-rich tract; blue, A-rich tract. Sequence before the poly(A) site is in lowercase letters, whereas sequence after the poly(A) site is in uppercase letters. 5-nt words containing at least four U and A residues were considered as U- and A-rich elements, respectively. Discontinuous line indicates that part of the nucleotide sequence has been omitted in order to shorten DNA sequences and evidence the conserved motifs. References for each gene are indicated at the right. (For interpretation of the references to colour in this figure legend, the reader is referred to the web version of the article.) (see refs. Binder et al. (1995), Bruchhaus et al. (1996), Deng et al. (1998), Edman et al. (1987, 1990), Huber et al. (1988), Leippe et al. (1992), López-Camarillo et al. (2003), Nozaki et al. (1998), Ramos et al. (1997), Riahi et al. (2004), Rodriguez et al. (1996), Sanchez and Muller (1998), Sanchez et al. (1994), Tachibana et al. (1991), Tannich et al. (1991a, 1991b) and Wostmann et al. (1992))

content of 3′-UTR. Although it is the only A-rich element detected among the top-10 motifs, we considered the AAAAA motif (8th) as relevant since other A-rich words were detected in the top-20 motifs (Supplementary Fig. 2). The search for 4-nt and 6-nt words did not identify other relevant motifs in genomic sequences (data not shown).

The most representative 5-nt words described above were all located throughout a 9-nt region (Fig. 2D): AU-rich motifs clustered from 26 to 29 nt position, overlapping with the U-rich elements that were centered on 28–29 nt position. The AAAAA pentamer is the more remote motif, being around the 35 nt position.

3.5. Detection of predicted cis-regulatory elements in E. histolytica genes with known poly(A) site

Results obtained from the computational study of EST and genomic sequences were assessed by a complementary analysis of 3′-end region from 19 *E. histolytica* genes with known poly(A) site (Fig. 3). The consensus polyadenylation signal UA(A/U)UU (or variant with one nt changed) was detected 8–25 nt upstream the poly(A) site in all sequences, excepted in the Ehserp gene. Interestingly, it was included in stop codon in four genes. The poly(A) site was denoted by the U residue in 11 genes. In 15 genes, it was surrounded by U-rich motifs (0–7 nt upstream and 0–9 nt downstream the poly(A) site). Finally, the novel A-rich region identified in this work was present at 9–44 nt downstream the poly(A) site in 95% of the sequences.

3.6. Predicted secondary structures of 3′-end regions from E. histolytica genes

We explored the formation of higher order structure for *E. histolytica* transcripts with known poly(A) site using the Quikfold program (Zuker, 2003; Markham and Zuker, 2005) (Fig. 4). For analysis purposes, the input was a 400-nt region where the poly(A) site was at the 300 nt position. Interestingly, secondary structures corresponding to a minimal free energy value (from −56.2 to −82.8 kcal mol^{-1}) could be clustered into two previously reported groups (Loke et al., 2005): the poly(A) site was located on a cluster of stem loop structures in 53% of transcripts (group I, represented by the Ehtub gene), whereas it was on or around the stem loop, but not flanked by a cluster of secondary structures, in 47% of transcripts (group II, represented by the Ehadh3 gene). Consequently, the stem loop structures found around the poly(A) site were obtained from base pairing of adjacent regions that contain *cis*-regulating elements for mRNA 3′-end formation (Fig. 4).

4. Discussion

In eukaryotic cells, mRNA polyadenylation is an important gene expression control point that depends on *trans*-acting factors interacting with specific 3′-UTR *cis*-acting elements. Considering that it is possible to predict regulatory elements based on their conserved position and nt content in a large set of sequences, several groups have reported the in silico identification of conserved elements that could be involved in mRNA poly(A) tail formation in *A. thaliana* (Loke et al., 2005), *H. sapiens* (Hu et al., 2005) and *S. cerevisiae* (Graber et al., 2002). To our knowledge, the present paper is the first report about the prediction of pre-mRNA 3′-UTR regulatory sequences in a protozoan parasite.

Our analysis of *E. histolytica* EST sequences evidenced that the last 25-nt region upstream the poly(A) site contains a AU-rich domain corresponding to the consensus UA(A/U)UU polydenylation signal or variants, followed by a U-rich region preceding the poly(A) site that is generally characterized the U residue. Data obtained from genomic sequences showed that the AU-rich region is located downstream the stop codon and upstream the poly(A) site, and evidenced the presence of a novel A-rich element that is located after the poly(A) site. Analysis of *E. histolytica* genes with known poly(A) site confirmed this hypothetical array and suggested that the U-rich region could surround the poly(A) site. The fact that the polyadenylation signal was included in the stop codon in

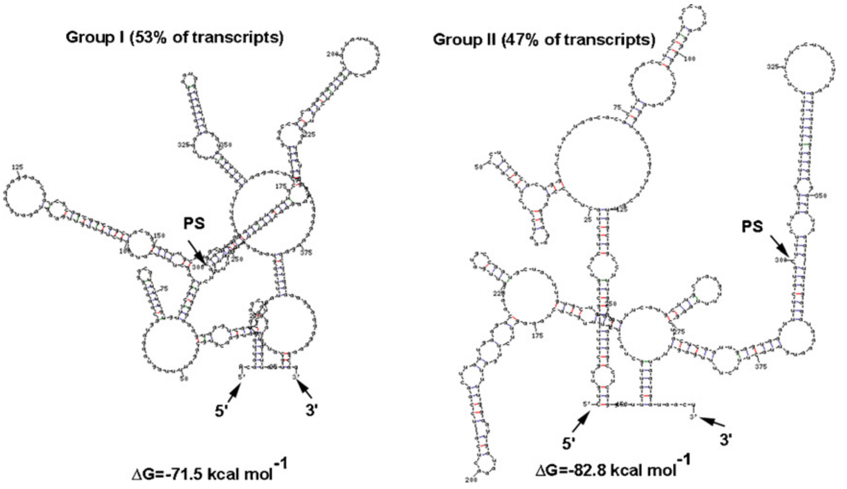

Fig. 4. Representative secondary structure predictions. For each gene with known poly(A) site (PS), a RNA fragment of 400 nt (where the poly(A) site was at position 300) was analyzed with the DINAMelt server (Markham and Zuker, 2005). Group I, PS is located on a cluster of stem loop structures; Group II, PS is on or around the stem loop, but it is not flanked with a cluster of secondary structures. 5′- and 3′-ends are indicated.

several genes may support the hypothesis that the stop codon is the polyadenylation signal ancestor, dividing the codifying and not codifying genetic regions.

The molecular organization of pre-mRNA 3′-end processing signals is roughly conserved through evolutionary scale (Fig. 5). *E. histolytica* presents a U-rich region preceding the poly(A) site, as in plants, human and yeast. Moreover, we detected another U-rich tract downstream the poly(A) site, as in plants, human, yeast and *T. vaginalis*. In addition, distances between each motif are in the same range in all organisms. Remarkably, the novel A-rich region downstream the poly(A) site, seems to be unique for *E. histolytica* transcripts. Interestingly, the polyadenylation signal is the conserved A(A/U)UAAA hexanucleotide in plants, animals and yeast, whereas it appears to be specie-specific in the few protozoan parasites studied, corresponding to AGU(A/G)AAA in *Giardia lamblia* (Peattie et al., 1989; Que et al., 1996), UAAA in *T. vaginalis* (Espinosa et al., 2002), AUUAAA in the *Plasmodium* pgs28 gene (Cann et al., 2004) and UA(A/U)UU in *E. histolytica* (Bruchhaus et al., 1993).

The high incidence of the canonical polyadenylation signal UA(A/U)UU in EST and genomic sequences, confirmed the functional relevance of this motif for pre-mRNA polyadenylation. The detection of UA(A/U)UU variants suggested that the core polyadenylation machinery of *E. histolytica* (López-Camarillo et al., 2005) could be able to interact with different polyadenyla-

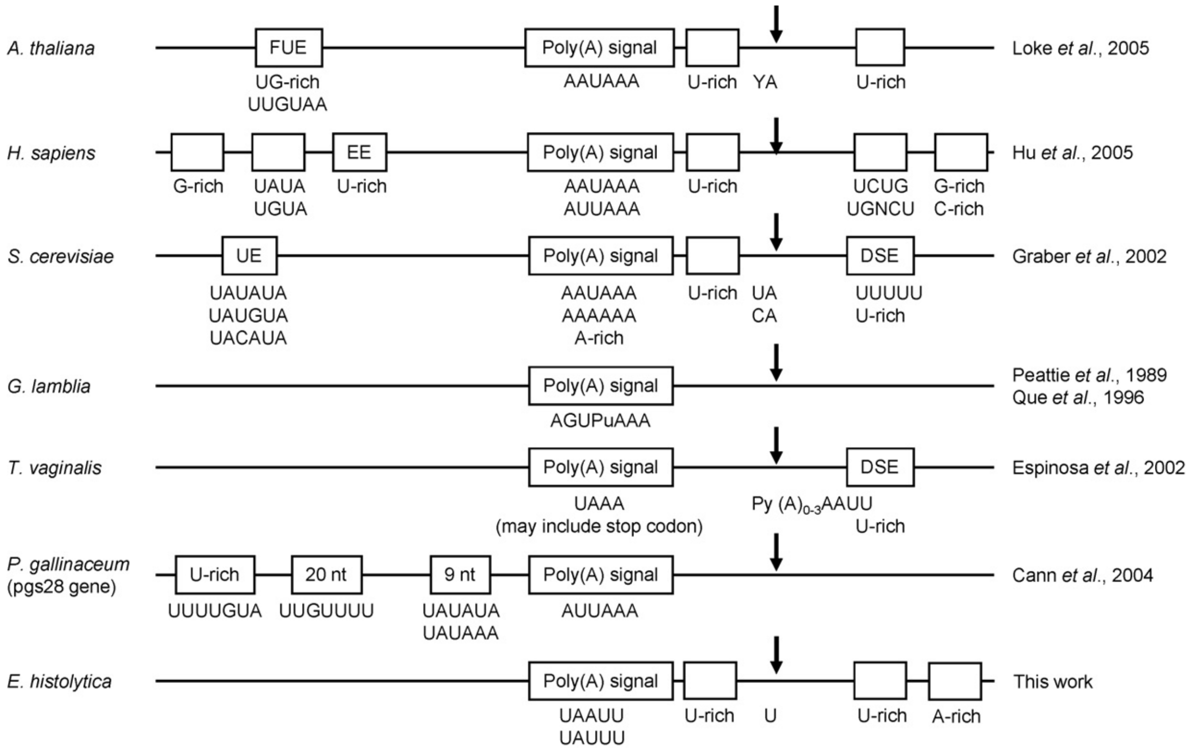

Fig. 5. Comparison of pre-mRNA 3′-UTR processing signals through evolutionary scale. DSE, downstream element; EE, efficiency element; FUE, far-upstream element; Arrow, poly(A) site. References are indicated at the right.

tion signals. In human, CPSF160 binding to the consensus AAUAAA polyadenylation signal is stimulated by CstF, indicating that CPSF160 alone could be able to recognize divergent polyadenylation signals (Wilusz et al., 1990). The U1-snRNP A-protein (Gunderson et al., 1998; Lou et al., 1998) and hnRNP-F/H (Veraldi et al., 2001) proteins have been reported as modulators of polyadenylation, regulating the selection of the consensus polyadenylation signal by the core polyadenylation factors. The presence of multiple polyadenylation signals in several sequences also suggested that the use of distinct polyadenylation signal could be an important regulatory event for *E. histolytica* gene expression. Additionally, our data suggested the existence of UA(A/U)UU-independent polyadenylation processes in *E. histolytica*, adding more complexity to mRNA 3′-end formation mechanism in this protozoan pathogen.

The prediction of RNA secondary structure by energy minimization was used to explore the topological association with functional signals. *E. histolytica* transcripts folding brings regulatory sequences closer together, probably facilitating interactions between the distinct factors of the pre-mRNA 3′-end processing machinery to perform the polyadenylation reaction. In other organisms, it has been reported that mutations in poly(A) signal reduced polyadenylation efficiency (Mogen et al., 1990; Rothnie et al., 1994), which was associated with structural changes in mRNA folding (Loke et al., 2005). Therefore, structural studies of RNA–protein interactions are of particular interest to understand the pre-mRNA 3′-end cleavage and polyadenylation process.

The present study showed the useful of computer-based methods to determine sequences with a potential role in biological process. Our data will contribute to the understanding of gene expression regulation in *E. histolytica*, providing new insights into pre-mRNA 3′-end polyadenylation mechanisms in this pathogen. The functional relevance of *E. histolytica* sequence elements identified here is currently under experimental investigation.

Acknowledgments

We thank Christiane Bouchier (Genopole at Pasteur Institute, France) for her help in automated cDNA sequencing. This work was supported by CONACyT, SIP-IPN, COFAA-IPN and UACM (Mexico).

Appendix A. Supplementary data

Supplementary data associated with this article can be found, in the online version, at doi:10.1016/j.compbiolchem.2008.03.019.

References

Beaudoing, E., Freier, S., Wyatt, J.R., Claverie, J.M., Gautheret, D., 2000. Patterns of variant polyadenylation signal usage in human genes. Genome Res. 10, 1001–1010.

Binder, M., Ortner, S., Plaimauer, B., Fodinger, M., Wiedermann, G., Scheiner, O., Duchene, M., 1995. Sequence and organization of an unusual histone H4 gene in the human parasite *Entamoeba histolytica*. Mol. Biochem. Parasitol. 71, 243–247.

Bruchhaus, M., Leippe, C., Lioutas, C., Tannich, E., 1993. Unusual gene organization in the protozoan parasite *Entamoeba histolytica*. DNA Cell Biol. 12, 925–933.

Bruchhaus, I., Jacobs, T., Denart, M., Tannich, E., 1996. Pyrophosphate-dependent phosphofructokinase of *Entamoeba histolytica*: molecular cloning, recombinant expression and inhibition by pyrophosphate analogues. Biochem. J. 316, 57–63.

Cann, H., Brown, S.V., Oguariri, R.M., Golightly, L.M., 2004. 3′ UTR signals necessary for expression of the *Plasmodium gallinaceum* ookinete protein, Pgs28, share similarities with those of yeast and plants. Mol. Biochem. Parasitol. 137, 239–245.

Deng, Z., Huang, M., Singh, K., Albach, R.A., Latshaw, S.P., Chang, K.P., Kemp, R.G., 1998. Cloning and expression of the gene for the active PPi-dependent phosphofructokinase of *Entamoeba histolytica*. Biochem. J. 329, 659–664.

Edman, U., Meza, I., Agabian, N., 1987. Genomic and cDNA actin sequences from a virulent strain of *Entamoeba histolytica*. Proc. Natl. Acad. Sci. U.S.A. 84, 3024–3028.

Edman, U., Meraz, M.A., Rausser, S., Agabian, N., Meza, I., 1990. Characterization of an immuno-dominant variable surface antigen from pathogenic and nonpathogenic *Entamoeba histolytica*. J. Exp. Med. 172, 879–888.

Espinosa, N., Hernandez, R., Lopez-Griego, L., Lopez-Villasenor, I., 2002. Separable potential polyadenylation and cleavage motifs in *Trichomonas vaginalis* mRNAs. Gene 289, 81–86.

Graber, J.H., McAllister, G.D., Smith, T.F., 2002. Probabilistic prediction of *Saccharomyces cerevisiae* mRNA 3′-processing sites. Nucleic Acids Res. 30, 1851–1858.

Gunderson, S.I., Polycarpou-Schwarz, M., Mattaj, I.W., 1998. U1 snRNP inhibits pre-mRNA polyadenylation through a direct interaction between U1 70K and poly(A) polymerase. Mol. Cell 1, 255–264.

Hajarnavis, A., Korf, I., Durbin, R., 2004. A probabilistic model of 3′ end formation in *Caenorhabditis elegans*. Nucleic Acids Res. 32, 3392–3399.

Hu, J., Lutz, C.S., Wilusz, J., Tian, B., 2005. Bioinformatic identification of candidate *cis*-regulatory elements involved in human mRNA polyadenylation. RNA 11, 1485–1493.

Huber, M., Garfinkel, L., Gitler, C., Mirelman, D., Revel, M., Rozenblatt, S., 1988. Nucleotide sequence analysis of an *Entamoeba histolytica* ferredoxin gene. Mol. Biochem. Parasitol. 31, 27–33.

Jackson, T.F., 2000. Epidemiology. In: Ravdin, J.I. (Ed.), Amebiasis. Imperial College Press, London, pp. 47–63.

Leippe, M., Tannich, E., Nickel, R., van der Goot, G., Pattus, F., Horstmann, R.D., Muller-Eberhard, H.J., 1992. Primary and secondary structure of the pore-forming peptide of pathogenic *Entamoeba histolytica*. EMBO J. 11, 3501–3506.

Loftus, B., Anderson, I., Davies, R., Alsmark, U.C., Samuelson, J., Amedeo, P., et al., 2005. The genome of the protist parasite *Entamoeba histolytica*. Nature 433, 865–868.

Loke, J.C., Stahlberg, E.A., Strenski, D.G., Haas, B.J., Wood, P.C., Li, Q.Q., 2005. Compilation of mRNA polyadenylation signals in *Arabidopsis* revealed a new signal element and potential secondary structures. Plant Physiol. 138, 1457–1468.

López-Camarillo, C., Luna-Arias, J.P., Marchat, L.A., Orozco, E., 2003. EhPgp5 mRNA stability is a regulatory event in the *Entamoeba histolytica* MDR phenotype. J. Biol. Chem. 278, 11273–11280.

López-Camarillo, C., Orozco, E., Marchat, L.A., 2005. *Entamoeba histolytica*: comparative genomics of the pre-mRNA 3′ end processing machinery. Exp. Parasitol. 110, 184–190.

Lou, H., Neugebauer, K.M., Gagel, R.F., Berget, S.M., 1998. Regulation of alternative polyadenylation by U1 snRNPs and SRp20. Mol. Cell. Biol. 18, 4977–4985.

Markham, N.R., Zuker, M., 2005. DINAMelt web server for nucleic acid melting prediction. Nucleic Acids Res. 33, 577–581.

Mogen, B.D., MacDonald, M.H., Graybosch, R., Hung, A.G., 1990. Upstream sequences other than AAUAAA are required for efficient messenger RNA 3′-end formation in plants. Plant Cell 2, 1261–1272.

Nozaki, T., Arase, T., Shigeta, Y., Asai, T., Leustek, T., Takeuchi, T., 1998. Cloning and bacterial expression of adenosine-5′-triphosphate sulfurylase from the enteric protozoan parasite *Entamoeba histolytica*. Biochim. Biophys. Acta 1429, 284–291.

Peattie, D.A., Alonso, R.A., Hein, A., Caulfield, J.P., 1989. Ultrastructural localization of giardins to the edges of disk microribbons of *Giardia lamblia* and the nucleotide and deduced protein sequence of alpha giardin. J. Cell. Biol. 109, 2323–2335.

Proudfoot, N., 2004. New perspectives on connecting messenger RNA 3′ end formation to transcription. Curr. Opin. Cell. Biol. 16, 272–278.

Que, X., Svard, S.G., Meng, T.C., Hetsko, M.L., Aley, S.B., Gillin, F.D., 1996. Developmentally regulated transcripts and evidence of differential mRNA processing in *Giardia lamblia*. Mol. Biochem. Parasitol. 81, 101–110.

Ramos, M.A., Salgado, L.M., Mercado, G.C., Sanchez-Lopez, R., Stock, R.P., Lizardi, P.M., Alagon, A., 1997. *Entamoeba histolytica* contains a gene encoding a homologue to the 54 kDa subunit of the signal recognition particle. Mol. Biochem. Parasitol. 88, 225–235.

Riahi, Y., Siman-Tov, R., Ankri, S., 2004. Molecular cloning, expression and characterization of a serine proteinase inhibitor gene from *Entamoeba histolytica*. Mol. Biochem. Parasitol. 133, 153–162.

Rodriguez, M.A., Baez-Camargo, M., Delgadillo, D.M., Orozco, E., 1996. Cloning and expression of an *Entamoeba histolytica* NAPD+(−)dependent alcohol dehydrogenase gene. Biochim. Biophys. Acta 1306, 23–26.

Rothnie, H.M., Reid, J., Hohn, T., 1994. The contribution of AAUAAA and the upstream element UUUGUA to the efficiency of mRNA 3′-end formation in plants. EMBO J. 13, 2200–2210.

Sanchez, L.B., Muller, M., 1998. Cloning and heterologous expression of *Entamoeba histolytica* adenylate kinase and uridylate/cytidylate kinase. Gene 209, 219–228.

Sanchez, M.A., Peattie, D.A., Wirth, D., Orozco, E., 1994. Cloning, genomic organization and transcription of the *Entamoeba histolytica* alpha-tubulin-encoding gene. Gene 146, 239–244.

Tachibana, H., Ihara, S., Kobayashi, S., Kaneda, Y., Takeuchi, T., Watanabe, Y., 1991. Differences in genomic DNA sequences between pathogenic and nonpathogenic isolates of *Entamoeba histolytica* identified by polymerase chain reaction. J. Clin. Microbiol. 29, 2234–2239.

Tannich, E., Bruchhaus, I., Walter, R.D., Horstmann, R.D., 1991a. Pathogenic and nonpathogenic *Entamoeba histolytica*: identification and molecular cloning of an iron-containing superoxide dismutase. Mol. Biochem. Parasitol. 49, 61–71.

Tannich, E., Scholze, H., Nickel, R., Horstmann, R.D., 1991b. Homologous cysteine proteinases of pathogenic and nonpathogenic *Entamoeba histolytica*. Differences in structure and expression. J. Biol. Chem. 266, 4798–4803.

Veraldi, K.L., Arhin, G.K., Martincic, K., Chung-Ganster, L.H., Wilusz, J., Milcarek, C., 2001. hnRNP F influences binding of a 64-kilodalton subunit of cleavage stimulation factor to mRNA precursors in mouse B cells. Mol. Cell. Biol. 21, 1228–1238.

Weber, C., Guigon, G., Bouchier, C., Frangeul, L., Moreira, S., Sismeiro, O., Gouyette, C., Mirelman, D., Coppee, J.Y., Guillen, N., 2006. Stress by heat shock induces massive down regulation of genes and allows differential allelic expression of the Gal/GalNAc lectin in *Entamoeba histolytica*. Eukaryot. Cell 5, 871–875.

Wilusz, J., Shenk, T., Takagaki, Y., Manley, J.L., 1990. A multicomponent complex is required for the AAUAAA-dependent cross-linking of a 64-kilodalton protein to polyadenylation substrates. Mol. Cell. Biol. 10, 1244–1248.

Wostmann, C., Tannich, E., Bakker-Grunwald, T., 1992. Ubiquitin of *Entamoeba histolytica* deviates in six amino acid residues from the consensus of all other known ubiquitins. FEBS Lett. 308, 54–58.

Zhao, J., Hyman, L., Moore, C., 1999. Formation of mRNA 3′ ends in eukaryotes: mechanism, regulation, and interrelationships with other steps in mRNA synthesis. Microbiol. Mol. Biol. Rev. 63, 405–445.

Zuker, M., 2003. Mfold web server for nucleic acid folding and hybridization prediction. Nucleic Acid Res. 31, 3406–3415.